Synthesis, Characterization, and Magnetic Properties of γ-Na$_x$CoO$_2$ ($0.70 \leq x \leq 0.84$)

Hiroya Sakurai[1]*, Satoshi Takenouchi[2], Naohito Tsujii[3], and Eiji Takayama-Muromachi[1]

[1] *Superconducting Materials Center, National Institute for Materials Science (SMC/NIMS), 1-1 Namiki, Tsukuba, Ibaraki 305-0044, Japan.*
[2] *Research Promotion Division, National Institute for Materials Science, 1-1 Namiki, Tsukuba, Ibaraki 305-0044, Japan.*
[3] *NanoMaterials Laboratory, National Institute for Materials Science (NML/NIMS), 1-2-1 Sengen, Tsukuba, Ibaraki 305-0044, Japan.*

Powder Na$_x$CoO$_2$ ($0.70 \leq x \leq 0.84$) samples were synthesized and characterized carefully by X-ray diffraction analysis, inductive-coupled plasma atomic emission spectroscopy, and redox titration. It was proved that γ-Na$_x$CoO$_2$ is formed only in the narrow range of $0.70 \leq x \leq 0.78$. Nevertheless, the magnetic properties depend strongly on x. We found, for the first time, two characteristic features in the magnetic susceptibility of Na$_{0.78}$CoO$_2$, a sharp peak at $T_\mathrm{p} = 16$ K and an anomaly at $T_\mathrm{k} = 9$ K, as well as the transition at $T_\mathrm{c} = 22$ K and the broad maximum at $T_\mathrm{m} = 50$ K which had already been reported. A type of weak ferromagnetic transition seems to occur at T_k. The transition at T_c, which is believed to be caused by spin density wave formation, was observed clearly for $x \geq 0.74$ with constant T_c and T_p independent of x. On the other hand, ferromagnetic moment varies systematically depending on x. These facts suggest the occurrence of a phase separation at the microscopic level, such as the separation into Na-rich and Na-poor domains due to the segregation of Na ions. The magnetic phase diagram and transition mechanism proposed previously should be reconsidered.

KEYWORDS: Na$_x$CoO$_2$, ICP, redox titration, solid solution, magnetic susceptibility, SDW, ferromagnetic, phase separation

The strongly correlated electron system (SCES) is one of the most interesting research subjects for condensed matter physicists because of its excellent characteristics such as unconventional superconductivity, metal-insulator transition, and giant magnetoresistance. Na$_x$CoO$_2$ has attracted attention as an SCES since the discovery of high thermoelectrical performance.[1,2] The number of research studies on this compound has increased recently because of the discovery of superconductivity in its analogue, Na$_x$CoO$_2\cdot y$H$_2$O.[3] γ-Na$_x$CoO$_2$ has a layered structure in which oxygen planes with a triangular lattice are stacked in an AABB sequence. Co and Na ions occupy the octahedral and prism sites, respectively. The CoO$_6$ octahedra share their edges forming CoO$_2$ layers with Co ions on a triangular lattice.

Many experimental studies on γ-Na$_x$CoO$_2$ have been performed, and the results have not always been consistent. Na$_{0.75}$CoO$_2$ shows a transition to the spin density wave (SDW) state at $T_\mathrm{c} = 22$ K,[4] which was confirmed by muon spin rotation/relaxation (μSR) measurement.[5] Although SDW usually causes an increase in electric resistivity, it drops just below T_c in the present compound. Motohashi *et al*. have proposed a mechanism that the resistivity drop is due to the elimination of one of two Fermi surfaces by the SDW formation,[4] based on the band calculation of Na$_{0.5}$CoO$_2$.[6] This anomaly at T_c has been reported by other groups[7,8] for samples with slightly different x values. However, neutron scattering measurements have shown that the dominant magnetic fluctuation is not antiferromagnetic, but ferromagnetic.[9] Furthermore, it has been suggested that this compound seems to be an itinerant electron system.[9] On the other hand, it has

been recently reported that no such transition is seen in the magnetic susceptibility of the $x = 0.75$ sample, which shows a broad maximum at 14 K,[10] or Curie-Weiss behavior (with a tiny kink at approximately 30 K probably caused by the secondary phase of Co$_3$O$_4$).[11]

The solid solution range of Na content has been reported to be narrow between x=0.65 and 0.78.[12] For a lower x of 0.5-0.7, however, almost all samples contained Co$_3$O$_4$ as an impurity phase, which showed a kink or a peak in the magnetic susceptibility at approximately 30-35 K. According to nuclear magnetic resonance (NMR) measurements, the resultant phase was always Na$_{0.7}$CoO$_2$ when the nominal x was lower than 0.7.[13] These results indicate that the solid-solution range terminates at $x \simeq 0.7$. In addition, Na$_{0.7}$CoO$_2$ may have a charge-ordered state of magnetic Co^{4+} ($3d^5$) and non-magnetic Co^{3+} ($3d^6$) at a low temperature as suggested by NMR,[13–15] although it shows metallic behavior below 300 K. It is suggested that the magnetic Co^{4+} ions induce Curie-Weiss behavior in the magnetic susceptibility.

It should be noted that recent research of the Na$_x$CoO$_2$ system is focused on the two end members of the solid solution with $x \simeq 0.7$ and $\simeq 0.78$. These members seem to have quite different physical properties with apparent itinerant-electron behavior for $x = 0.75$, and with localized-electron behavior for $x = 0.7$. On the other hand, a dome-shaped magnetic phase diagram with x as a variable has been proposed[16,17] in spite of no experimental data between $x = 0.65$ and 0.75. In the present study, we synthesized Na$_x$CoO$_2$ samples and investigated their magnetic properties systematically.

The powder samples of Na$_x$CoO$_2$ ($x = 0.70, 0.72, 0.74, 0.76, 0.78, 0.80, 0.82,$ and 0.84) were synthesized

by conventional solid state reaction from the stoichio-metric mixture of Na_2CO_3 (99.99%) and Co_3O_4 (99.9%), which were dried at 300°C before use. The mixture was cold-pressed into a pellet, and in order to avoid possible vaporization of Na, the surface-to-volume ratio of the pellet was reduced and the heating process was carried out carefully. More concretely, the amount of each mixture was about 12 g and the mixture was pressed into several pellets with a diameter of 15 mm. The pellets were placed in a dense aluminous crucible and heated in flowing oxygen gas three times at $T_{\mathrm{syn}} = 800$, 850 and 950°C with intermediate grindings. The increase rate of temperature was 5°C/min up to 100°C below T_{syn} and was reduced to 20°C/h for the last 100°C increase to minimize Na vaporization. The sample was maintained at T_{syn} for 6 h and cooled in the furnace. In the final heat treatment at 950°C, cooling rate was controlled; it took 2 h from 950 to 850°C, 1 h from 850 to 750°C, 6 h at 750°C for annealing, and 12 h from 750 to 350°C. We tried to synthesize $Na_{0.67}CoO_2$ but a single-phase sample could not be obtained even after heating several times. The grain sizes of the present samples seemed to vary less compared with those made by the rapid heating technique.[18] The obtained samples were kept in an evacuated desiccator to prevent absorption of water in air.

The samples were characterized by powder X-ray diffraction (XRD) analysis, inductive-coupled plasma atomic emission spectroscopy (ICP-AES) and redox titration. XRD analysis was carried out using a Bragg-Brentano-type diffractometer (RINT2200HF, Rigaku) with Cu K_α radiation. Lattice constants were calculated from several peaks in the range of $5° \leq 2\theta \leq 60°$. ICP-AES was carried out by dissolving the sample in hydrochloric acid to determine the ratio of Na to Co, x. In the redox titration, each sample was dissolved in hydrochloric acid with an excess amount of $(COONa)_2$ as a reducing agent, and residual $(COONa)_2$ was titrated using a standard aqueous solution of $KMnO_4$. The Co valence, s, was estimated from the result of the titration using the weight ratio determined by ICP-AES.

The magnetic properties of the powder samples were measured using a commercial magnetometer with a superconducting quantum interference device (MPMS-XL, Quantum Design). Before each measurement under zero-field cooling (ZFC) conditions, the magnetic field was reset to 0 Oe at $T = 100$ K or 300 K. In this paper, we simply define magnetic susceptibility as $\chi = M/H$ (M: magnetization, and H: applied magnetic field).

All XRD peaks were assignable to γ-Na_xCoO_2 for every sample. However, this does not necessarily mean only a single phase was present, because a possible secondary phase such as Na_2CO_3 or NaOH is hard to detect by XRD analysis. Indeed, in Fig. 1(a), the lengths of the a- and c-axes vary with x below $x \sim 0.78$ but are constant for x above 0.78, strongly suggesting the higher solution limit of $x=0.78$.

The results of ICP-AES and the redox titration are shown in Fig. 1(b). The ratio of Na to Co, x, determined by ICP-AES is in good agreement with the nominal value even for a higher x range. This means that Na was not va-
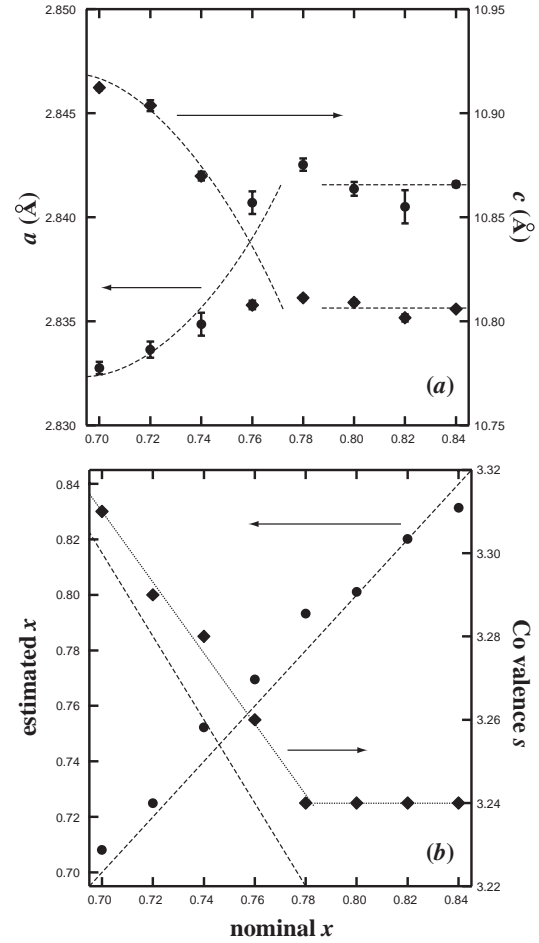

Fig. 1. (a) Lattice constants, a (the circles) and c (the squares), of Na_xCoO_2. The broken lines are visual guides. (b) Ratio of Na to Co, x, estimated by ICP-AES (the circles) and the formal valence of Co, s, estimated by the redox titration (the squares). The broken lines are the ideal x and s expected from the nominal x. The dotted lines are the fitting results (see the text).

porized in our synthetic process. Ideally, the Co valence, s, should obey the line, $s = 4 - x$, but experimental data are placed on the line, $s = 3.9 - 0.85x$, below $x = 0.78$. Above $x = 0.78$, the Co valence has the constant value of 3.24. The two lines have a difference of ~ 0.01 in s which seems to be beyond the accuracy of our titration experiment and may be due to a certain systematic error. Nevertheless, we believe that the almost constant Co valences above $x = 0.78$ reflect the solution limit of $x=0.78$. The synthesis experiment is consistent with the solid solution range of 0.70 - 0.78 in x and this is supported by the magnetic measurements (see below).

The T-dependences of χ of $Na_{0.78}CoO_2$ are shown in Fig. 2. There are four characteristic features: (1)the sharp transition at $T_C = 22$ K, (2) a fairly sharp peak at $T_P = 16$ K of FC curves under $H \leq 100$ Oe, (3) a broad maximum at $T_m = 50$ K, and (4) an anomaly at approximately $T_k = 9$ K which is seen as an upturn under a low magnetic field while as a dull downward kink under a high magnetic field of 10 kOe $\leq H \leq$ 30 kOe.

The transition at T_C has been reported by Motohashi et al^4 to be due to SDW formation. T_C is completely independent of H as seen Fig. 2. This transition and the

Fig. 2. (a) Temperature dependence of magnetic susceptibility of $Na_{0.78}CoO_2$ measured under various magnetic fields. The inset shows the M-H curve at 1.8 K. The solid line is $M = -3.18 \times 10^{-4} + 1.55 \times 10^{-7} H$. (b) Expanded graph of (a). The χ-T curves are off-set to be distinguished.

Fig. 3. Magnetic susceptibilities of Na_xCoO_2 measured under 10 kOe (a) and 100 Oe (b). The closed and open circles represent the susceptibilities and reciprocal susceptibilities, respectively.
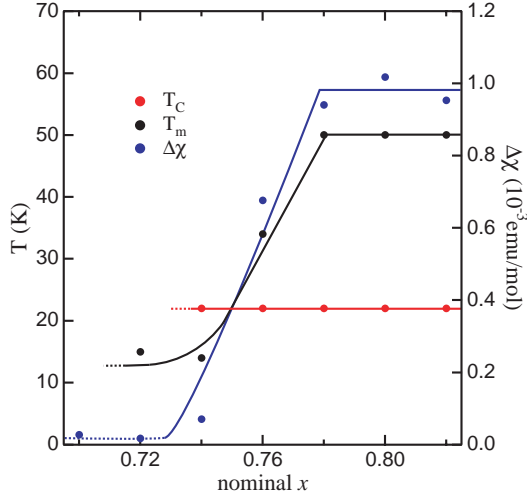

Fig. 4. Characteristic parameters, T_C (red), T_m (black), and $\Delta\chi$ (blue). The lines are visual guides.

hysteresis between ZFC and FC curves are also observed in other samples with $x \geq 0.74$, but is most prominent for $x = 0.78$, less pronounced with decreasing x, and almost invisible for $x \leq 0.72$ as seen in Fig. 3(b). However, T_C is independent of x, which means that the magnetic phase diagram does not have a dome shape as suggested by Sugiyama et al.[16,17]

T_p is also independent of x as seen in Fig. 3(b). On the other hand, the difference in χ under 100 Oe between ZFC and FC data at T_p, $\Delta\chi$, increases systematically with increasing x as seen in Fig. 4. These strongly suggest that the phase responsible for the transition in question does not change but only its fraction varies with x. Thus, we considered a phase separation to explain these phenomena. A phase separation into Na-rich and Na-poor domains seems to be the most probable and the transition at T_C takes place only in the former domain whose fraction increases with x. This idea is consistent with the specific heat measurement[19] and with the results of μSR which indicate that the volume fraction of magnetic domain is only $\sim$21% in the case of $x = 0.75$.[5] The transition has been observed in a single crystal[8] and the phase separation seems to occur at the microscopic level which cannot be detected by XRD analysis.

T_m depends on x as seen in Figs. 3(a) and 4. One may think that the broad maximum at T_m is due to the SDW fluctuation, namely short-range or intralayer ordering. However, the χ of $x = 0.74$ clearly shows $T_m < T_C$,

which indicates that the broad maximum has no relation with the transition at T_C. The x dependence suggests that this behavior is caused by domains that survive the phase separation. T_m may correspond to a characteristic temperature below which a heavy Fermi-liquid state develops, as discussed previously.[10]

The data between 150 K and 320 K were fit using the Curie-Weiss law with a constant term. The Curie constants were approximately 0.16 emu·K/Co mol with an effective moment of $\simeq 1.1\ \mu_B$. Assuming an ionic model with local moments caused by a low-spin configuration, only Co^{4+} ions have the magnetic moment of $S = 1/2$. Then, the Curie constant and effective moment of the Co^{4+} ions are calculated to be 0.62 emu·K/Co^{4+} mol and 2.2 μ_B, which almost agrees with the expected value of 1.7 μ_B in consideration of the deviation of the g-factor from 2. The Weiss temperature is approximately -120 K, from which one may assume antiferromagnetic interaction. However, ferromagnetic fluctuation has been observed by neutron inelastic scattering for $Na_{0.75}CoO_2$ and the compound is suggested to be an itinerant electron system.[9] Band calculation has also pointed out its itinerant ferromagnetic tendency.[6] Thus, the negative Weiss temperature could be due to the Curie-Weiss behavior of itinerant electrons with a small exchange enhancement factor,[20] namely this compound behaves like a nearly ferromagnetic metal, at least, at the high-temperature region. Many itinerant electron systems show Curie-Weiss behavior with Curie constants expected from the local moments.[21–23]

The upturns of the ZFC curves under $H \leq 5$ kOe below T_k appear to be due to a paramagnetic impurity. However, the upturns become less pronounced with increasing H, and become dull downward kinks under 10 kOe $\leq H \leq$ 30 kOe (see Fig. 2(b)). This phenomenon cannot be explained by magnetic impurities. Thus, it seems that the anomaly is due to a weak ferromagnetic transition like that observed at T_C. Indeed, preliminary specific heat measurements show an anomaly at T_k in the case of $x \geq 0.74$.[19] The anomaly is not seen for the sample with $x \leq 0.72$. On the other hand, for $H = 50$ kOe and 70 kOe, the magnetic phase is probably different from that for $H \leq 30$ kOe; the M-H curve at 1.8 K bends at approximately $H \simeq 40$ kOe as seen in the inset of Fig. 2(a).

There is no marked change in magnetic properties between $x = 0.70$ and 0.78. This suggests the lack of change in the electronic state, although the models of itinerant electrons and local moments have been proposed for lower and higher x values, respectively.[9,13–15] On the other hand, the magnetic properties for $x \geq 0.80$ are the same as those for $x = 0.78$, which is very consistent with the solid solution limit of $x = 0.78$ determined in the synthesis experiments.

Finally, we will discuss the possibility of two types of Fermi surface with one being insensitive to carrier density. Although such a situation may explain the present magnetic phenomena without assuming phase separation, the presence of only one type of Fermi surface is very likely for $x > 0.7$ according to the results of the band calculation of the $x = 0.5$ phase[6] and angle-resolved

photoemission spectroscopy.[24, 25] Here, it is worth noting that the electric resistivity of the present system drops below T_c and that the phenomenon has been explained assuming the two types of Fermi surfaces. It seems that another reason needs to be found for the resistivity drop. Moreover, the peak in the χ-T curve at T_p is not caused by simple SDW formation. In order to elucidate the physical properties of the system in more detail, research to obtain microscopic information such as NMR is indispensable and is in progress.

In conclusion, we synthesized powder samples of $Na_x CoO_2$ ($0.70 \leq x \leq 0.84$) and characterized them carefully by XRD analysis, ICP-AES, and redox titration. It was proved that γ-$Na_x CoO_2$ can be obtained for the narrow range of $0.70 \leq x \leq 0.78$. Nevertheless, the magnetic properties of this system depend strongly on x. We have found, for the first time, two characteristic features of the magnetic susceptibility of $Na_{0.78}CoO_2$, the sharp peak at $T_p = 16$ K and an anomaly at $T_k = 9$ K, as well as a transition at $T_c = 22$ K and a broad maximum at T_m which were previously reported. A kind of weak ferromagnetic transition seems to take place at T_k. The transition at T_c, which is believed to be due to SDW formation, is clearly observed for $x \geq 0.74$ with fixed T_c and T_p independent of x. Ferromagnetic moment decreases systematically with decreasing x. These suggest a type of phase separation, such as that into Na-rich and Na-poor domains. The magnetic phase diagram and mechanism of the transition proposed thus far should be reconsidered.

Acknowledgements

1) I. Terasaki, Y. Sasago and K. Uchinokura: Phys. Rev. B **56** (1997) R12685.
2) I. Terasaki: Physica B **328** (2003) 63.
3) K. Takada, H. Sakurai, E. Takayama-Muromachi, F. Izumi, R. A. Dilanian and T. Sasaki: Nature (London) **422** (2003) 53.
4) T. Motohashi, R. Ueda, E. Naujalis, T. Tojo, I. Terasaki, T. Atake, M. Karppinen and H. Yamauchi: Phys. Rev. B **67** (2003) 064406.
5) J. Sugiyama, H. Itahara, J. H. Brewer, E. J. Ansaldo, T. Motohashi, M. Karppinen and H. Yamauchi: Phys. Rev. B **67** (2003) 214420.
6) D. J. Singh: Phys. Rev. B **61** (2000) 13397.
7) D. Prabhakaran, A. T. Boothroyd, R. Coldea, L. M. Helme and D. A. Tennant: cond-mat/0312493.
8) S. Bayrakci, C. Bernhard, D. P. Chen, B. Keimer, R. K. Kremer, P. Lemmens, C. T. Lin, C. Niedermayer and J. Strempfer: Phys. Rev. B **69** (2004) 100410(R).
9) A. T. Boothroyd, R. Coldea, D. A. Tennant, D. Prabhakaran, L. M. Helme and C. D. Frost: Phys. Rev. Lett. **92** 197201.
10) K. Miyoshi, E. Morikuni, K. Fujiwara, J. Takeuchi and T. Hamasaki: Phys. Rev. B **69** (2004) 132412.
11) P. Carretta, M. Mariani, C. B. Azzoni, M. C. Mozzati, I. Bradarić, I. Savić, A. Feher and J. Šebek: cond/mat/0312284.
12) J. B. Goodenough, K. Mizushima and T. Takeda: Jpn. J. Appl. Phys. **19** (1980) 305.
13) I. R. Mukhamedshin, H. Alloul, G. Collin and N. Blanchard: cond-mat/0402074.
14) R. Ray, A. Ghhoshray, K.Ghoshray and S. Nakamura: Phys. Rev. B **59** (1999) 9454.
15) J. L. Gavilano, D. Rau, B. Pedrini, J. Hinderer, H. R. Ott, S. Kazakov and J. Karpinski: Phys. Rev. B **69** (2004) 100404(R).
16) J. Sugiyama, J. H. Brewer, E. J. Ansaldo, H. Itahara, T. Tani, M. Mikami, Y. Mori, T. Sasaki, S. Hébert and A. Maignan: Phys. Rev. Lett. **92** (2004) 017602.
17) J. Sugiyama, J. H. Brewer, E. J. Ansaldo, B. Hitti, M. Mikami, Y. Mori and T. Sasaki: cond-mat/0310637.
18) T. Motohashi, E. Naujalis, R. Ueda, K. Isawa, M. Karppinen and H. Yamauchi: Appl. Phys. Lett. **79** (2001) 1480.
19) H. Sakurai, N. Tsujii and E. Takayama-Muromachi: unpublished data.
20) T. Moriya: *Spin Fluctuations in Itinerant Electron Magnetism* (Springer-Verlag, Berlin, Heidelberg, New York and Tokyo, 1985).
21) I. Felner, I. Nowik and D. Shaltiel: Solid State Comm. **40** (1981) 1073.
22) M. Takigawa and H. Yasuoka: J. Phys. Soc. Jpn. **51** (1982) 787.
23) Y. Takahashi and T. Moriya: J. Phys. Soc. Jpn. **54** (1985) 1592.
24) M. Z. Hasan, Y.-D. Chuang, A. P Kuprin, Y. Kong, D. Qian, Y. W. Li, B. L. Mesler, Z. Hussain, A. V. Fedorov, R. Kimmerling, E. Rotenberg, K. Rossnagel, H. Koh, M. Rogado, M. L. Foo and R. J. Cava: cond-mat/0308438.
25) H.-B. Yang, S.-C. Wang, A. K. P. Sekharan, H. Matsui, S. Souma, T. Sato, T. Takahashi, T. Takeuchi, J. C. Campuzano, R. Jin, B. C. Sales, D. Mandrus, Z. Wang and H. Ding: cond-mat/0310532.

This figure "Fig2R.gif" is available in "gif" format from:

http://arXiv.org/ps/cond-mat/0407613v1

This figure "Fig3R.gif" is available in "gif" format from:

http://arXiv.org/ps/cond-mat/0407613v1